JACS
JOURNAL OF THE AMERICAN CHEMICAL SOCIETY

ARTICLE

pubs.acs.org/JACS

Can Ferric-Superoxide Act as a Potential Oxidant in $P450_{cam}$? QM/MM Investigation of Hydroxylation, Epoxidation, and Sulfoxidation

Wenzhen Lai and Sason Shaik

Institute of Chemistry and The Lise Meitner-Minerva Center for Computational Quantum Chemistry, The Hebrew University of Jerusalem, 91904 Jerusalem, Israel

Supporting Information

ABSTRACT: In view of recent reports of high reactivity of ferric-superoxide species in heme and nonheme systems (Morokuma et al. J. Am. Chem. Soc. 2010, 132, 11993−12005; Que et al. Inorg. Chem. 2010, 49, 3618−3628; Nam et al. J. Am. Chem. Soc. 2010, 132, 5958−5959; J. Am. Chem. Soc. 2010, 132, 10668−10670), we use herein combined quantum mechanics/molecular mechanics (QM/MM) methods to explore the potential reactivity of $P450_{cam}$ ferric-superoxide toward hydroxylation, epoxidation, and sulfoxidation. The calculations demonstrate that P450 ferric-superoxide is a sluggish oxidant compared with the high-valent oxoiron porphyrin cation-radical species. As such, unlike heme enzymes with a histidine axial ligand, the P450 superoxo species does not function as an oxidant in $P450_{cam}$. The origin of this different behavior of the superoxo species of P450 vis-à-vis other heme enzymes like tryptophan 2, 3-dioxygenase (TDO) is traced to the ability of the latter superoxo species to make a stronger FeOO−X (X = H,C) bond and to stabilize the corresponding bond-activation transition states by resonance with charge-transfer configurations. By contrast, the negatively charged thiolate ligand in the P450 superoxo species minimizes the mixing of charge transfer configurations in the transition state and raises the reaction barrier. However, as we demonstrate, an external electric field oriented along the Fe−O axis with a direction pointing from Fe toward O will quench Cpd I formation by slowing the reduction of ferric-superoxide and will simultaneously lower the barriers for oxidation by the latter species, thereby enabling observation of superoxo chemistry in P450. Other options for nascent superoxo reactivity in P450 are discussed.

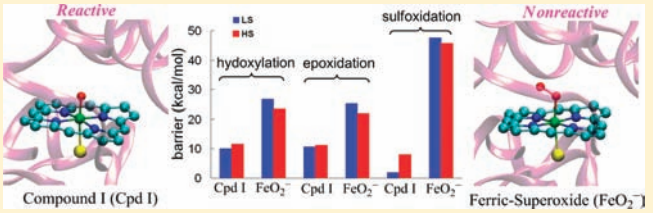

1. INTRODUCTION

Despite the recent breakthrough in the preparation and characterization of the high-valent iron-oxo species, so-called compound I (Cpd I) of cytochrome P450,[1,2] in high enough yields that allowed following its reactivity, there is still some uncertainty over *the exclusivity of this reactive species* in carrying out the key oxidative processes of the enzymes and their mutants.[3−5] The catalytic cycle of P450, shown in Scheme 1, displays a few iron−oxygen species that can potentially act as reactive oxygen species. It is widely accepted that the P450 cycle begins with a resting state, **1**, where a water molecule occupies the distal coordination site of iron. The entry of the substrate into the active site expels the water ligand and produces a pentacoordinated ferric complex, **2**. Then, reduction of the ferric state to the ferrous species, **3**, followed by O_2 uptake forms the ferric-superoxo species, $Fe^{III}-OO^-$, **4**, which undergoes a second reduction to yield ferric-peroxy, $Fe^{III}-OO^{2-}$, **5**, which upon protonation generates the ferric-hydroperoxo species, $Fe^{III}-OOH$, **6**, so-called compound 0 (Cpd 0). The latter undergoes an additional protonation event on the distal oxygen and liberates a water molecule, thus resulting in the formation of Cpd I, **7**.

Among all these species, Cpd I is considered to be the ultimate oxidant that is responsible for the single most important reaction catalyzed by P450s, the incorporation of an oxygen atom into organic substrates, for example, C−H hydroxylation, C=C epoxidation, sulfoxidation, etc.[3−5] However, seminal mechanistic studies[6−10] suggested that both **5** and **6** could also be involved in catalysis of the various oxidative processes. The Cpd 0 species, **6**, has been invoked even as a competitor of Cpd I in the key reaction of oxygen incorporation, for example, C−H hydroxylation, C=C epoxidation, and sulfoxidation. While theory supports the role of **5** as a strong nucleophilic species in deformylation transformation of aldehydes,[11] it does not support the involvement of **6** as either an oxidant[12−14] or a nucleophile.[11] This conclusion has also partial support from experimental data on P450,[15] as well as on nonheme $Fe^{III}-OOH$ species.[16] As such, this leaves us with an open ended question: *Is there another oxygen species that can function as an oxidant in the P450 cycle*?

Consideration of the current literature[17,18] underscores the potential of ferric-superoxide, **4**, as a likely candidate that may compete with Cpd I or replace it as the reactive oxygen species in mutated enzymes where the disrupted protonation machinery prevents or delays Cpd I formation.[4a] Indeed, recently, many studies have revealed that the superoxo species of enzymes and synthetic models *are highly reactive* and sometimes even more so than the iron-oxo species. These studies cover heme enzymes,[17,18] nonheme enzymes,[19−23] and some synthetic analogues.[24−27] Specifically, in their study of the oxidative cleavage of the pyrrole ring of L-tryptophan by the ferric-superoxide of tryptophan

Received: December 17, 2010
Published: March 17, 2011

dx.doi.org/10.1021/ja111376n | J. Am. Chem. Soc. 2011, 133, 5444–5452

Scheme 1. The Catalytic Cycle of P450

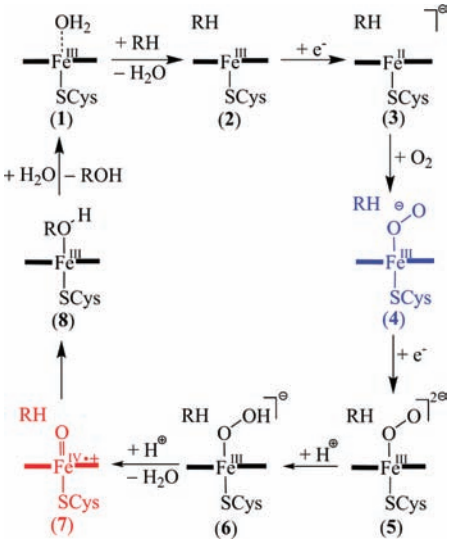

Scheme 2. (a) Reactions, (b) Oxidants Used in the QM/MM model, and (c) Oxidants and Substrates in the QM-Only Calculations

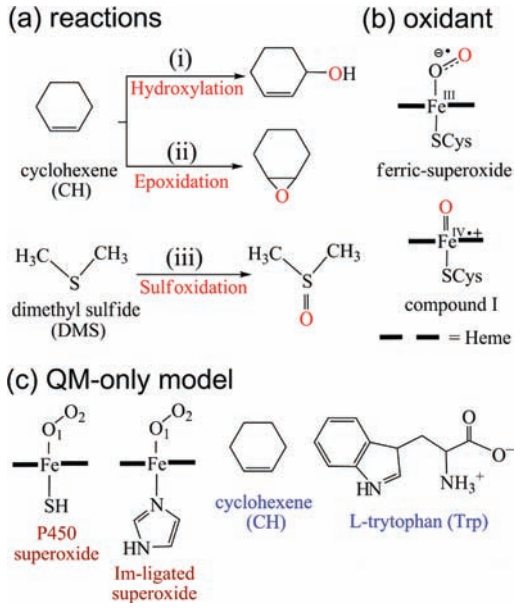

2,3-dioxygenase (TDO), Morokuma et al.[17b] also reported the relative energy of bond activation transition states for ferric-superoxo attacks on small π systems and suggested the ferric-superoxo species is capable of reacting with π systems via direct radical addition. This finding raises naturally some questions: What is the situation in P450? Can ferric-superoxide compete with Cpd I in P450?

To answer these questions, we investigate herein three types of reactions (Scheme 2a), hydroxylation and epoxidation of cyclohexene (CH) and sulfoxidation of dimethyl sulfide (DMS), by means of quantum mechanical/molecular mechanical (QM/MM) calculations. For each type of reaction, both ferric-superoxide and Cpd I species of $P450_{cam}$ (Scheme 2b) are considered as potential oxidants, and their relative reactivities are assessed. To compare P450 with TDO, we also investigated the reactions of ferric-superoxide with CH and tryptophan (Scheme 2c) by means of QM-only calculations. As shall be shown, in the wild-type P450, ferric-superoxide gives high reaction barriers and hence cannot compete with Cpd I. Furthermore, the imidazole (Im) ligand of TDO is found to endow the ferric-superoxo with a higher reactivity compared with the corresponding P450 species. However, as we demonstrate, mutations or external electric fields (EEF),[28] which quench the second electron transfer process that converts **4** to **5**, may reveal a P450 superoxo reactivity.

2. THE COMPUTATIONAL METHODS

2.1. Setup of the System. *2.1.1. Setup for the $P450_{cam}$ + CH Systems.* For the $P450_{cam}$/CH system, several snapshots were used in our previous QM/MM study.[29] Accordingly we selected herein one snapshot, that is, snapshot 0, which gave the lowest hydroxylation and epoxidation barriers due to the barrier-lowering effect[30] of the liberated water molecule during the formation of Cpd I (Scheme 1). A detailed description of the setup has appeared in our recent papers[29] and is briefly described herein. Initial geometry was constructed from the X-ray structure (PDB code 1DZ9),[31a] which has an oxo ligand corresponding to the Cpd I species.[31b] No MM minimization was done on the enzyme itself before the QM/MM calculations were started. The same protonation state of the protein as before was considered.[28,29] To model ferric-superoxide, **4** (Figure 1), the distal ligand group was replaced by O_2, and the water molecule (Wat903) that is liberated only after formation of Cpd I was removed.

2.1.2. Setup for $P450_{cam}$ + DMS Systems. The initial structures for the QM/MM calculations were taken from the corresponding $P450_{cam}$ + CH systems and the CH substrate was replaced by DMS.

2.2. QM/MM Methodology and Software. QM/MM calculations were done with ChemShell,[32] combining Turbomole[33]/DL_POLY.[34] An electronic embedding scheme[35] was applied to include the polarizing effect of the enzyme environment on the QM region. Hydrogen link atoms with the charge-shift model[36] were used to treat the QM/MM boundary. The CHARMM22 force field[37] was employed throughout this study for the MM part. The QM part was treated with the hybrid B3LYP functional[38] as implemented in Turbomole (in which the fifth form of VWN local correlation functional is used). Based on previous experience with C−H and C═C activations,[3,29] geometry optimization for the reactions with CH was carried out with a double-ζ basis set LACVP[39] for iron and 6-31G for all other atoms, labeled as B1c, while the energy was corrected by single-point calculations with a larger basis set B2c, involving LACV3P+*[40] for all the atoms. For the reactions with DMS, B1c yields a sulfoxide product with an overly long S−O bond (see Figure S2 and S3 in the Supporting Information), and hence, as done in the past,[3,41,42] geometry optimization employed the LACVP** (B1s) basis set, and the energy was corrected by single-point calculations with a larger basis set B2s, involving LACV3P++** for all the atoms. In addition, B1c was shown to be appropriate even for the negatively charged superoxo and peroxo species.[3] Nevertheless, we tested the influence of a larger basis set, LACVP+*, on the singlet species in reactions by ferric-superoxide and found negligible effects on the geometries and barriers (barriers change within 0.5 kcal/mol compared with the results with B2c//B1c; for details see Part I of Supporting Information). All QM/MM energy scans were performed by going forward and backward to ascertain contiguous energy profiles.

B3LYP has been repeatedly shown capable of reproducing both experimental and high-level computational results for P450.[3] However,

dx.doi.org/10.1021/ja111376n |J. Am. Chem. Soc. 2011, 133, 5444–5452

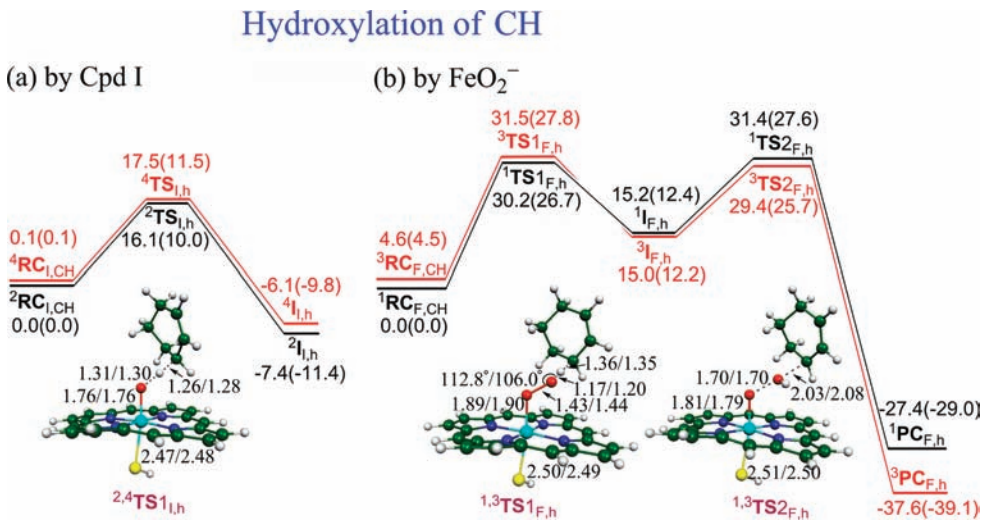

Figure 1. Calculated QM/MM energy profiles (in kcal/mol) for hydroxylation of CH by (a) Cpd I and (b) ferric-superoxide. The relative energies correspond to B3LYP(B3LYP-D), respectively, using the B2c basis set.

in the specific case of O_2 binding to hemes, B3LYP deviates significantly from the experimental results, due to lack of primarily dispersion effects. Indeed, B3LYP with dispersion correction (B3LYP-D)[43] was found to give more accurate binding energies.[44] In the present work, all QM/MM calculations were preformed with the Turbomole 6.1 package, which includes the implementation of dispersion corrections for energy and gradients and hence allows us to test geometry optimization effects of the B3LYP-D level. As such, we performed B3LYP-D geometry optimizations with B1c for the first step of hydroxylation and epoxidation of CH by Cpd I and ferric-superoxide and found only minor effects on the geometry of TSs and the barriers, compared with the corresponding values that arose from B3LYP optimization followed by single-point dispersion correction (see Part II in the Supporting Information). Therefore, we use the B3LYP functional for geometry optimizations and upgrade the energies by single-point B3LYP-D calculations on B3LYP-optimized structures at the larger basis set (B2c or B2s) level.

The QM region contains iron−porphyrin (without side chains of the heme) with distal oxygen or dioxygen ligand, sulfur of Cys357, and full substrate. The optimized active region is similar to the one in our recent paper,[29] which involves heme and its distal ligand, full substrate, Pro86, Phe87, Tyr96, Pro100, Thr101, Gln108, Arg112, Leu244, Gly248, Asp251, Thr252, Val295, Asp297, Arg299, Phe350, His355, Leu356, Cys357, Leu358, Gly359, Gln360, Ile395, Val396, Wat61, Wat92, Wat265, and Wat903 if it is present.

For each reaction, the two lowest-lying spin states were investigated. The full set of data is summarized in the Supporting Information, while herein we focus on the key results.

2.3. QM/MM/EEF Studies. The effect of external electric fields (EEFs) on the reactivity of both Cpd I and superoxide was studied using the previously described methodology[28] to create EEFs with a desired strength by adding appropriate point charges (q_i) on two circular plates flanking the enzyme. To construct a uniform electric field, all the q_i should be the same, and the point charges on one side of the heme are mirrored on the other with opposite charges (the total number of generated point charges is 7082). These charged circular plates having radii of 92.4 Å were placed at distances of 46.8 Å from iron. These charges are treated along with the intrinsic MM charges of the enzyme during the QM/MM procedures. To gauge the effect of EEF on reactivity, we preformed single-point calculations (using the larger B2c basis set) for the reactant clusters (RCs) and TSs for H-abstraction and direct radical addition reactions in the $P450_{cam}$/CH system (for details see Part VII in the Supporting Information).

2.4. QM Studies. The reactions of ferric-superoxide having imidazole ligand with CH and tryptophan were compared with those of the corresponding P450 species. Geometry optimizations and vibrational frequency calculations were done at the B3LYP/B1c level using Gaussian 09,[45] and the energies were corrected with B2c by single-point calculations using Jaguar 7.6.[46] To obtain reliable charge distribution, we carried out the natural bonding orbital (NBO) analysis using NBO 3.1 program[47] implemented in Gaussian 09 at the B1c level.

3. RESULTS

3.1. Hydroxylation of CH. In the case of hydroxylation by Cpd I, hydrogen abstraction is generally considered to be the rate-determining step, while the rebound[48] step is much faster.[3,49] Therefore, only the H-abstraction step was considered herein, while the details of the rebound can be found elsewhere.[3] We have previously investigated the hydroxylation vs epoxidation of CH by $P450_{cam}$ using an older version of Turbomole.[29] For the sake of consistency, we reoptimized the stationary points in the hydroxylation and epoxidation (discussed in section 3.2) pathways using the new version, Turbomole 6.1, which leads to minor changes only (on geometries and relative energies).

Figure 1 displays the energy profiles for the hydroxylation of CH by the ferric-superoxide and Cpd I, as well as the optimized geometries for transition states (TSs). The calculations revealed an expected two-state reactivity (TSR) scenario for Cpd I[50] and for the first time also for a heme ferric-superoxo species of P450. Note also that in the reactions of the superoxide, we describe the entire hydroxylation mechanism, since this is the first such study for P450.

3.1.1. Hydroxylation of CH by Cpd I. It is clear that the H-abstraction reaction of Cpd I with CH (the subscript I in the various species denotes Cpd I) exhibits nearly degenerate triradicaloid low-spin (LS) doublet and high-spin (HS) quartet states. B3LYP predicts a H-abstraction barrier of 16.1/17.4 kcal/mol for the doublet/quartet state. Dispersion correction lowers the two barriers by 6 kcal/mol to 10.0/11.4 kcal/mol, respectively. Such significant barrier-lowering effects of dispersion correction were discussed recently by Lonsdale et al.[51] In the H-abstraction TSs, ^{2}**TS**$_{I,h}$/^{4}**TS**$_{I,h}$ (the subscript h denotes hydroxylation), the

dx.doi.org/10.1021/ja111376n |*J. Am. Chem. Soc.* 2011, 133, 5444–5452

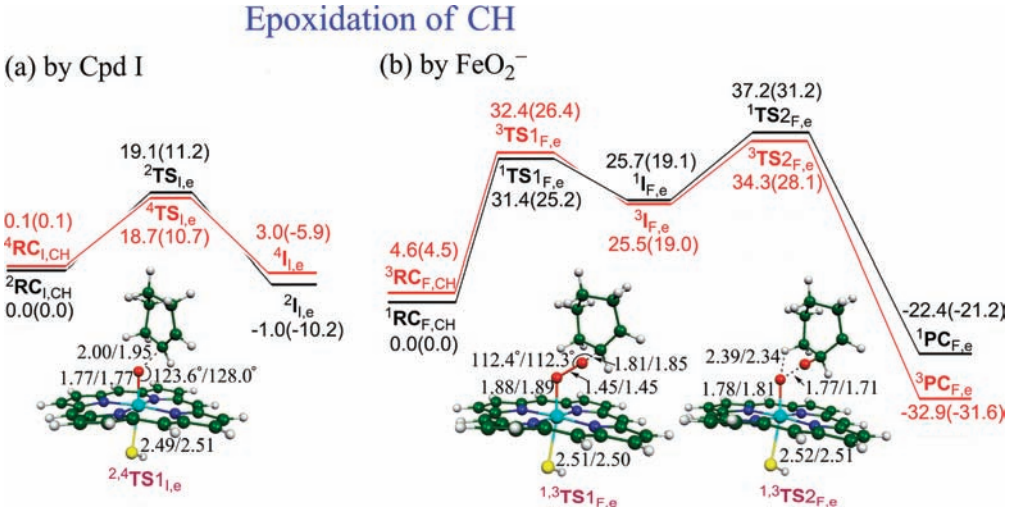

Figure 2. Calculated QM/MM energy profile (in kcal/mol) for hydroxylation of CH by (a) Cpd I and (b) ferric-superoxide. The relative energies are noted as B3LYP (B3LYP-D) values using the B2c basis set.

transferred hydrogen atom is midway between O and C, r_{OH} = 1.31/1.30 Å and r_{CH} = 1.26/1.28 Å. Applying the zero-point energy correction from the gas-phase calculations (−3.4/−3.6 kcal/mol) will result in B3LYP-D barriers of 6.6/7.8 kcal/mol. If we use these barriers in the Eyring equation, they would correspond to rate constants of $\sim 10^6$−10^8 s^{-1}, in reasonable accord with experimental estimates of high rates for P450.[1]

3.1.2. Hydroxylation of CH by Ferric-Superoxide

3.1.2.1. Mechanism. The reaction of the ferric-superoxide in Figure 1b starts at the reactant cluster, $\mathbf{RC}_{F,CH}$ (the subscript F denotes the ferric-superoxide). The ferric-superoxide complex has two low-lying states,[52,53] an open-shell LS singlet is the ground state, which is 4.6 kcal/mol (B3LYP) lower than the triplet state. B3LYP-D predicts similar singlet−triplet splitting (4.5 kcal/mol).

As shown in the figure, the hydroxylation by the ferric-superoxide is stepwise. It starts with a hydrogen abstraction step and is followed by concerted O−OH cleavage and OH transfer to the cyclohexenyl radical to form the C−OH bond leading to cyclohexenol and a ferryl-oxo species (compound II = Cpd II). To estimate the barrier for the latter step, we performed a two-dimensional QM/MM scan, in which we employed the forming O−C bond and the breaking O−O bond as two scanning coordinates (Figure S6 in the Supporting Information). A stepwise mechanism comprising of homolytic O−O bond breaking followed by C−OH bond formation was found to have higher barrier and was hence relegated to the Supporting Information.

3.1.2.2. The Hydrogen Abstraction Step in the Reaction of Ferric-Superoxide. The B3LYP energetic barrier for this reaction is 30.2/26.9 kcal/mol for the singlet/triplet state. B3LYP-D lowers these barriers by 3−4 kcal/mol to 26.7/23.3 kcal/mol. Addition of zero-point energy correction (−3.7/−3.7 kcal/mol) from the gas-phase calculations results in barriers of 23.0/19.6 kcal/mol. Much like in H-abstraction by Cpd I, here too the so-generated states of the Cpd 0/substrate−radical complex are nearly degenerate. In contrast to the exothermicity of H-abstraction by Cpd I, herein the H-abstraction is endothermic. In the H-abstraction TSs, $^1\mathbf{TS1}_{F,h}/^3\mathbf{TS1}_{F,h}$, the transferred hydrogen atom is closer to the acceptor-oxygen atom than to the donor-carbon atom: r_{OH} = 1.17/1.20 Å and r_{CH} = 1.36/1.35 Å, while ∠CHO = 112.8°/106.0°.

3.1.2.3. The C−OH Bond Formation Step for the Reaction of Ferric-Superoxide. Starting from $^{1,3}\mathbf{I}_{F,h}$ in Figure 1b, single-point QM (B3LYP)/MM calculation at the B2c level from the two-dimensional scan of this step gives estimated activation energies of 16.2/14.4 kcal/mol for the singlet/triplet state. B3LYP-D gives similar barriers of 15.2/13.5 kcal/mol for the singlet/triplet. Relative to the $^{1,3}\mathbf{I}_{F,h}$ intermediates, the C−OH bond formation step is highly exothermic, −41.4/−51.3 kcal/mol (B3LYP-D).

3.2. Epoxidation of CH by Cpd I and Ferric-Superoxide. Figure 2 displays the energy profiles for the epoxidation of CH by Cpd I and ferric-superoxide, along with the optimized geometries for the transition states.

3.2.1. Epoxidation of CH by Cpd I. The reaction mechanism of the epoxidation by Cpd I was studied before and found to exhibit two distinct phases, that is, the C═C bond activation and the C−O rebound phases.[54] Since the first phase is the rate-determining step, herein we only studied this bond activation step. B3LYP predicts C═C bond activation barriers of 18.7/19.0 kcal/mol for doublet/quartet state. However, as shown recently by Lonsdale et al.[51] and found herein too, inclusion of dispersion correction lowers the barriers for epoxidation by 8 kcal/mol. Addition of zero-point energy correction (−0.5/−0.1 kcal/mol) from the gas-phase calculations results in epoxidation barrier of 10.2/11.0 kcal/mol at B3LYP-D/B2c for the doublet/quartet state, respectively.

Note that B3LYP predicts reaction energies of −1.0/2.9 kcal/mol for the doublet/quartet state, while B3LYP-D gives −10.2/−6.0 kcal/mol. It is clear that the dispersion correction causes 8−9 kcal/mol decrease in both reaction barriers and energies, which highlights the very significant effect of van der Waals interactions.[43,44,51,55,56] Additionally, in accord with the previous findings of Lonsdale et al.,[51] here too, the addition of dispersion corrections lowers the epoxidation barriers of CH more than the corresponding H-abstraction barriers. Thus, our zero-point energy corrected B3LYP-D barriers of 6.6/7.8 kcal/mol for hydroxylation and 10.2/11.0 kcal/mol for epoxidation in the doublet/quartet state are comparable to the gas phase values of

dx.doi.org/10.1021/ja111376n |J. Am. Chem. Soc. 2011, 133, 5444–5452

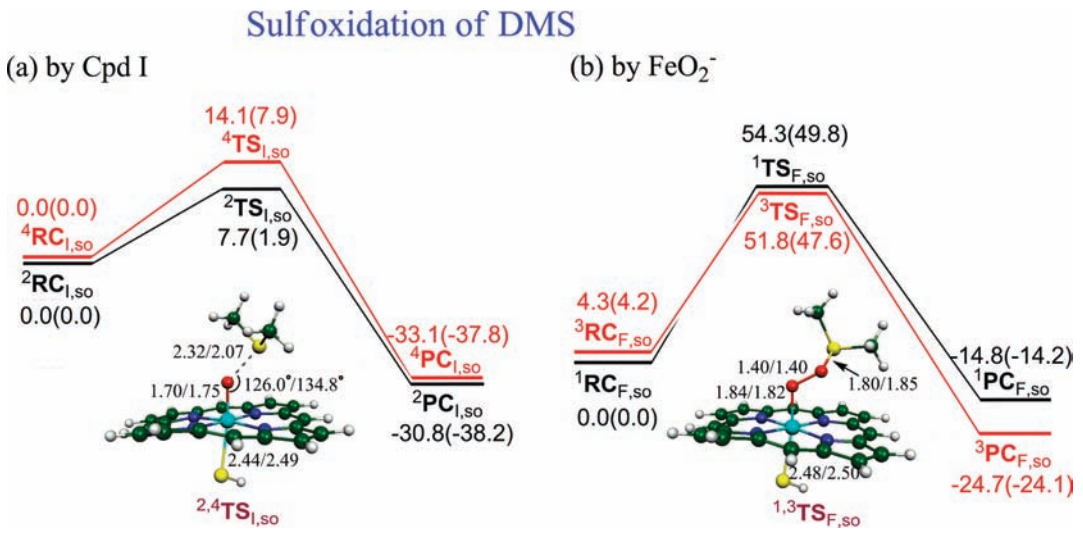

Figure 3. Calculated QM/MM energy profile (in kcal/mol) for sulfoxidation of DMS by (a) Cpd I and (b) ferric-superoxide. The relative energies are noted as B3LYP (B3LYP-D) values, respectively, at the B2s level.

Lonsdale et al.[51] of 7.7/6.7 kcal/mol and 9.4/7.7 kcal/mol, respectively.

3.2.2. Epoxidation of CH by Ferric-Superoxide. Much like the hydroxylation, the epoxidation process by ferric-superoxide, in Figure 2b, involves two distinct phases. Initially, in the bond activation phase, the distal oxygen atom of the ferric-superoxide attacks the terminal carbon atom of the double bond to form a C−O bond with the carbon atom of CH and a radical center on the adjacent carbon position. In a subsequent phase, the O−O bond breaks, along with a spontaneous epoxide ring closure. The mechanism herein is similar to the one found for the epoxide formation from the ferric-superoxide intermediate in typotophan 2,3-dioxygenase (TDO).[17b]

3.2.2.1. The C═C Activation Phase. As shown in Figure 2b, the B3LYP energies of transition states for C−O bond formation are 31.4 and 32.4 kcal/mol higher than $^1\mathbf{RC}_{F,CH}$ for the singlet and triplet states and ∼1 kcal/mol higher than those for H-abstraction. The dispersion correction lowers the barriers by about 6 kcal/mol making them approximately 1.5 kcal/mol lower than those for the corresponding H-abstraction (Figures 2b vs 1b). Addition of the zero-point energy correction (−0.5/−0.5 kcal/mol) from the gas-phase calculations results in B3LYP-D barrier of 24.7/21.4 kcal/mol for the singlet/triplet state, respectively.

The intermediate complex ($\mathbf{I}_{F,e}$) has degenerate singlet and triplet states, which lie 19.0 and 19.1 kcal/mol (B3LYP-D values) higher than $^1\mathbf{RC}_{F,CH}$, underscoring the high endothermicity of the bond activation step. In the C═C activation transition state, the O−C distance is 1.81/1.85 Å for the singlet/triplet state, which is 0.2/0.1 Å shorter than that in the C═C activation by Cpd I. This O−C distance decreases to 1.52/1.52 Å in the intermediate $^1\mathbf{I}_{F,e}/^3\mathbf{I}_{F,e}$.

3.2.2.2. The Epoxide Formation Phase for Ferric-Superoxide. As may be seen from Figure 2b, the O−O bond cleavage occurs with simultaneous O−C bond formation to give the epoxide and ferryl-oxo intermediates (Cpd II). For this step, B3LYP predicts a barrier of 11.5/8.8 kcal/mol for singlet/triplet state, while B3LYP-D leads to a similar result (12.1/9.1 kcal/mol). In contrast to the endothermicity of the first activation phase, the second phase here is highly exothermic (B3LYP-D value of 40.3/50.6 kcal/mol for the singlet/triplet state relative to the intermediate state).

3.3. Sulfoxidation of DMS by Cpd I and Ferric-Superoxide. Figure 3 displays the energy profiles for sulfoxidation of DMS by Cpd I and ferric-superoxide, as well as the optimized geometries for the corresponding transition states. Our QM/MM calculations show that Cpd I reacts via the doublet spin state, while ferric-superoxide tends toward two-state reactivity.

3.3.1. Sulfoxidation of DMS by Cpd I. The reaction proceeds in a single step (Figure 3a), with activation barriers of 7.7/14.1 kcal/mol and exothermicities of −30.8/−33.1 kcal/mol for the doublet/quartet state at B3LYP/B2s. After adding dispersion correction, the activation barrier decreases to 1.9/7.9 kcal/mol. The much lower barrier for the LS process follows our previous analysis, which showed that this and other two-electron processes should proceed preferentially via the LS state.[3,57] In the doublet/quartet transition state, the S−O distance is 2.32/2.07 Å, which is similar to the value from the gas-phase calculations (2.34/2.03 Å).[42]

We note that the present QM/MM preference for doublet state reaction is consistence with previous gas-phase calculations.[42] However, recent QM/MM (ONIOM) results by Porro et al.[12] preferred the quartet state reaction and gave a significantly higher barrier for the doublet state (20.0 vs 7.7 kcal/mol here). The higher barrier of Porro et al.[12] seems to be caused by the different TS geometry located in their study, but since the QM/MM methods used there are different than the present ones, we cannot further comment on the precise source of differences.

3.3.2. Sulfoxidation of DMS by the Ferric-Superoxide. The sulfoxidation of DMS by the ferric-superoxide proceeds through a concerted reaction, that is, the S−O bond formation is accompanied by O−O bond cleavage to generate sulfoxide and Cpd II (for details, see Figure S8 in the Supporting Information). The calculated barriers are ∼50 kcal/mol for both singlet and triplet spin states, which are much higher than those for the process catalyzed by Cpd I. In the singlet/triplet transition state, the S−O distance is 1.80/1.85 Å, while the O−O distance is 1.40/1.40 Å. It is clear that the S−O distance is shorter than that in the case of sulfoxidation by Cpd I. An interesting feature is that the S−O/O−O distances are comparable to the C−O/O−O distances in the TSs for epoxidation of CH.

dx.doi.org/10.1021/ja111376n |*J. Am. Chem. Soc.* 2011, 133, 5444–5452

Table 1. B3LYP-D/B2c Calculated Gas-Phase Barriers ($\Delta E^{\ddagger}$), Reaction Energies (ΔE),[a] and Amounts of Charge Transfer (Q_{CT}) for the Reactions of the P450 (L = SH^-) and the Imidazole-Ligated (L = Im) Superoxides in the Singlet/Triplet States

			B3LYP		B3LYP-D		
Fe−O_2^- species	substrate	reaction type	$\Delta E^{\ddagger}$	ΔE	$\Delta E^{\ddagger}$	ΔE	Q_{CT} (e^-)
L = SH^-	CH	H-abstraction	24.1/22.1	13.5/10.5	20.2/18.1	10.6/7.5	0.28/0.27
		C=C activation	27.2/25.4	20.5/17.3	22.4/20.7	15.4/12.3	0.18/0.18
	Trp	C=C activation	27.6/26.1	14.4/12.4	21.3/19.9	6.7/4.6	0.31/0.31
L = Im	CH	H-abstraction	20.7/17.5	10.1/5.2	17.6/14.9	7.9/3.0	0.34/0.32
		C=C activation	23.0/18.3	15.6/10.2	18.6/14.7	11.8/6.5	0.26/0.26
	Trp	C=C activation	20.6/17.6	11.3/7.6	13.6/11.0	1.5/-2.3	0.40/0.40

[a] In kcal/mol with zero-point energy correction.

3.4. External Electric Field (EEF) Effects on the Reactions of Cpd I and Superoxide with CH. Recently, we showed that an EEF aligned with the axis perpendicular to the porphyrin plane (F_z) can control the rate of the second electron transfer step, which converts superoxo **4** to **5**, *and is rate-determining for P450$_{cam}$*.[28] Specifically, an EEF along the $+z$ direction (pointing from Fe to O) was found to quench this electron transfer step and will therefore slow or altogether block the reduction of the superoxo and the eventual formation of Cpd I. Hence, it is interesting to establish whether the $+z$ EEF can at the same time enhance the reactivity of the ferric-superoxo species. Using F_z = +0.01 au, we found that the barriers for H-abstraction and C=C activation by superoxide were lowered by about 4 and 6 kcal/mol, respectively. Since the application of a $+z$ EEF was predicted[28] to obstruct the formation of Cpd I, its application on P450 may indeed reveal superoxo reactivity. Interestingly, the barriers for Cpd I reactivity are also lowered by the EEF, and in the $+z$ direction, C=C activation is slightly more favorably affected compared with H-abstraction. However, since the $+z$ EEF obstructs the formation of Cpd I, only an in situ generated Cpd I can reveal this reactivity effect.

3.5. QM Studies of the Reactions of Superoxide with CH and Tryptophan. To gauge the relative reactivity of the P450 superoxide vis-à-vis an imidazole-ligated superoxide (as in an enzyme like TDO), we computed the QM barriers and reaction energies for the reactions with CH and tryptophan. The data are displayed in Table 1 (for more details, see the Supporting Information). It is seen that the barriers of the imidazole-ligated superoxide are smaller than those for the P450 superoxo species. While this trend coincides with the smaller reaction endothermicities of the imidazole-ligated reactions, still the barriers are too much affected by the changes of thermodynamics. This requires a physical explanation that is deferred to the discussion section. A probe that will be helpful for understanding this effect is the amount of charge transfer, Q_{CT}, from the substrate to the oxidant in the transition state, which is seen from Table 1 to be consistently larger in the transition states of the imidazole-ligated superoxide.

4. DISCUSSION

Can ferric-superoxide act as a potential oxidant in P450? To answer this title question, we should compare the computed reaction barriers for ferric-superoxide to the corresponding ones for Cpd I. This is done in Figure 4, which summarizes the calculated B3LYP-D barriers for the first step of all the studied reactions. It is seen that while the barriers for both hydroxylation and epoxidation of cyclohexene found here for the ferric-superoxide are not exceedingly high, they are still higher than those of Cpd I, and the corresponding sulfoxidation barrier is very much higher. Therefore, Figure 4 shows clearly that by comparison to Cpd I, which is a powerful oxidant with low barriers, the P450 ferric-superoxo species is a sluggish oxidant and is not likely to affect the chemistry of wild-type P450s. Note that these barriers are not activation free energies, which require extensive sampling.[58] Nevertheless, judging from the recent study of sampling for H-abstraction by Cpd I of P450$_{cam}$,[58b] the sampling effect is small (1.2 kcal/mol or less) and hence will not affect the present conclusions, which are based on large differences.

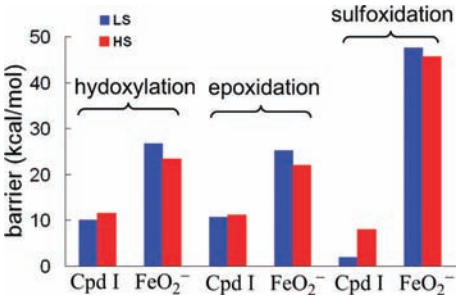

Figure 4. Calculated B3LYP-D activation barriers for the first step of each type of reaction.

What is the reason for the sluggish reactivity of P450 superoxide compared with the corresponding Cpd I? One immediate answer is found in the relative reaction energies of the corresponding bond activation processes. As seen from Figures 1−3, the reactions of the superoxo species are either endothermic or weakly exothermic compared with those by Cpd I, which are significantly exothermic. For example, the H-abstraction reaction of superoxide is 15 kcal/mol endothermic compared with the 7 kcal/mol exothermicity of the corresponding reaction of Cpd I, and the same is true for the C=C bond activation step. Thus, the FeO−H/FeO−C bonds are stronger than the FeOO−H/FeOO−C bonds, and following the Bell−Evans−Polanyi (BEP) principle,[59−62] we might expect the higher reactivity for Cpd I compared with the superoxo species. Indeed, the barrier heights and reaction energies for the reactions of Cpd I and ferric-superoxide with CH correlate linearly with each other (Figure S9 in the Supporting Information), as expected from the BEP principle.

The root cause of the stronger O−X (X = H,C) bonds generated in the reactions of Cpd I, compared with the OO−X bonds in the reactions of ferric-superoxide, can be traced to the

dx.doi.org/10.1021/ja111376n |J. Am. Chem. Soc. 2011, 133, 5444–5452

Scheme 3. Spin Density (ρ) Distribution in (a) Cpd I (7) and (b) Ferric-Superoxide (4)

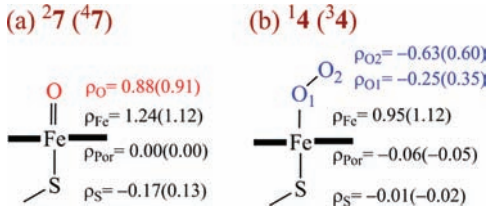

odd electron density on the oxygen atom that forms the bond. Generally, the higher the odd electron density on the attacking O-site, the more localized the radical, and the stronger will its O−X or OO−X bonds be.[63] Scheme 3 compares the spin densities for Cpd I vis-à-vis ferric-superoxide, and it is apparent that the oxo ligand has a significantly larger spin density than the distal oxygen of the superoxo ligand, wherein the spin density is delocalized over the two oxygen atoms. This delocalization of the odd electron is lost when the superoxide makes the OO−X bond either with H or with C, thereby causing less exothermic or more endothermic processes vis-à-vis Cpd I.

It is interesting to compare the P450 superoxide barriers to those in other enzymes. Thus, the H-abstraction barriers found here are around 20 kcal/mol higher than the one (Cys-β-C−H bond of the tripeptide substrate) calculated for the ferric-superoxo species of the nonheme isopenicylin *N* synthase (IPNS) enzyme.[21] Similarly, the epoxidation barriers of the P450 superoxide are also higher than the ones found by Morokuma et al.[17b] in their study of the oxidative cleavage of the pyrrole ring of L-tryptophan by the heme ferric-superoxide of tryptophan 2,3-dioxygenase (TDO), wherein they also reported relative energies of transition states for ferric-superoxo attacks on small π systems, which demonstrated that ferric-superoxo is capable of easily reacting with π systems. It appears therefore that imidazole-ligated ferric-superoxide is more reactive than the corresponding P450 species.

As noted in section 3.5 and in Table 1, there are two major factors for the higher reactivity of imidazole-ligated ferric-superoxo reagents:

(a) The reactions of the imidazole-ligated ferric-superoxide are less endothermic than those of the P450 species.

(b) The amount of charge transfer, Q_{CT}, from the substrate to the oxidant in the transition states (TSs) are always larger for the TSs of the imidazole-ligated superoxide (Table 1, last column). As argued recently,[60] a larger Q_{CT} value in the TS means that the corresponding TS enjoys increased resonance stabilization due to mixing of charge-transfer (ionic) configurations. As such, Table 1 shows that the TSs for the reactions of the imidazole-ligated superoxide are consistently more stabilized by resonance with the charge transfer state compared with the corresponding TSs in the P450 superoxo reactions. This is especially so in the case of the C=C addition reaction of tryptophan by imidazole-ligated superoxide, wherein the Q_{CT} values in the TSs are 0.40. These large Q_{CT} values indicate a strong mixing of charge-transfer configurations[60] and hence significant resonance stabilization of the corresponding TSs.

The factor that determines the relative Q_{CT} values for the two superoxo species types is their electron attachment energies (i.e., electron affinities), which are significantly affected by the electronic properties of the axial ligand.[64] Thus the negatively charged P450 superoxide has a much smaller electron attachment energy (electron affinity), as expected by considering the "push effect" of the thiolate ligand.[65] It follows that, by virtue of thermodynamics and electrostatic mismatch, *the thiolate ligand retards the reactivity of P450 ferric-superoxide, compared with systems wherein the axial ligand is imidazole (histidine).*

There is however, another and a major functional difference between P450 and IPNS or TDO, in terms of what transpires after the formation of the ferric-superoxo species in the dioxygenases (IPNS and TDO) vs P450. Thus, IPNS and TDO lack the appropriate reductive and protonation machineries (see Scheme 1 above) that convert the ferric-superoxide eventually to Cpd I, while in P450 these machineries exist and their ultimate function is to form Cpd I. Clearly, if and only if the disruption of the protonation pathway prevents reduction and formation of Cpd I, only then will P450 ferric-superoxide compete with Cpd I or replace it as an oxidant in the mutants. The recent QM/MM studies of Cpd I formation in various T252X (X = Ser, Val, Ala, Gly) and D251N mutants of $P450_{cam}$[66,67] show that this is unlikely to be the case; the O−O cleavage and formation of Cpd I in these mutants have barriers of the order of 14−19 kcal/mol, whereas the H-abstraction barriers computed herein exceed 20 kcal/mol. Thus, changing the protonation machinery cannot bring about nascent superoxo reactivity. However, our results suggest that mutations that slow the second electron transfer in the cycle (Scheme 1), which is known to be rate-controlling, may stop the $P450_{cam}$ cycle at the ferric-superoxo stage and lead to observation of superoxo oxidative chemistry and a detectable Cpd II species. This may be achieved by mutating the P450 residues at the site of attachment of the reductase (putidaredoxin in $P450_{cam}$) or by using an EEF.[28] *In the latter case, the EEF will quench Cpd I formation and enhance ferric-superoxo reactivity.*

5. CONCLUSIONS

The above QM/MM study on hydroxylation and epoxidation of cyclohexene and sulfoxidation of dimethyl sulfide by the ferric-superoxide and Cpd I of $P450_{cam}$ shows that ferric-superoxide is a sluggish oxidant compared with Cpd I. As such, the P450 superoxo species cannot function as an additional oxidant in $P450_{cam}$. This behavior is contrasted with the recently reported significant reactivity of superoxo species of the heme enzymes like TDO[17] and nonheme systems.[19,25,26] The origins of this different behavior are analyzed and traced to the greater ability of the latter superoxo species to make stronger FeOO−X (X = H,C) bonds and to stabilize the corresponding transition states by resonance with charge-transfer configurations. The negative charge of the P450 species minimizes the stabalizing effect of charge transfer in the transition state and contributes thereby to the sluggish reactivity of the superoxo species. However, as we demonstrate, an EEF oriented along the Fe−O axis with a direction pointing from Fe toward O will on the one hand quench Cpd I formation, by slowing the reduction of ferric-superoxide, and on the other lower the barriers for oxidation by the latter species, thereby enabling a possible observation of superoxo oxidative chemistry in P450. Notably, the existing capabilities to immobilize enzymes[68−71] suggest that the attachment of $P450_{cam}$, for example, to an electrode surface,[68,69] by use of self-assembled monolayers (SAMs) of bifunctional alkenthiols with anionic end groups (e.g., PO_3−SAM and CO_2−SAM),

dx.doi.org/10.1021/ja111376n |*J. Am. Chem. Soc.* 2011, 133, 5444–5452

which can link to the surface lysines at the distal site of the protein, may serve to orient the enzyme vis-à-vis the EEF and enable one thereby to study the potential reactivity of ferric-superoxide of P450.

■ ASSOCIATED CONTENT

Supporting Information. Complete citations for references 32, 37, and 45 and spin distribution, energies, and geometries of all the structures. This material is available free of charge via the Internet at http://pubs.acs.org.

■ AUTHOR INFORMATION

Corresponding Author
sason@yfaat.ch.huji.ac.il

■ ACKNOWLEDGMENT

This work was supported by the Israel Science Foundation (Grant ISF 53/09 to S.S.).

■ REFERENCES

(1) Rittle, J.; Green, M. T. *Science* **2010**, *330*, 933–937.
(2) Sligar, S. G. *Science* **2010**, *330*, 924–925.
(3) Shaik, S.; Cohen, S.; Wang, Y.; Chen, H.; Kumar, D.; Thiel, W. *Chem. Rev.* **2010**, *110*, 949–1017.
(4) (a) Denisov, I. G.; Makris, T. M.; Sligar, S. G.; Schlichting, I. *Chem. Rev.* **2005**, *105*, 2253–2277. (b) Sono, M.; Roach, M. P.; Coulter, E. D.; Dawson, J. H. *Chem. Rev.* **1996**, *96*, 2841–2888. (c) Ortiz de Montellano, P. R.; de Voss, J. J. *Nat. Prod. Rep.* **2002**, *19*, 477–493.
(5) Vaz, A. D. N. *Curr. Drug. Metab.* **2001**, *2*, 1–16.
(6) (a) Roberts, E. S.; Vaz, A. D. N.; Coon, M. J. *Proc. Natl. Acad. Sci. U.S.A.* **1991**, *88*, 8963–8966. (b) Vaz, A. D. N.; Roberts, E. S.; Coon, M. J. *J. Am. Chem. Soc.* **1991**, *113*, 5886–5887.
(7) (a) Coon, M. J.; McGinnity, D. F.; Vaz, A. D. N. *Proc. Natl. Acad. Sci. U.S.A.* **1998**, *95*, 3555–3560. (b) Coon, M. J.; Vaz, A. D. N.; Mcginnity, D. F.; Peng, H. M. *Drug Metab. Dispos.* **1998**, *26*, 1190–1193. (c) Toy, P. H.; Newcomb, M.; Coon, M. J.; Vaz, A. D. N. *J. Am. Chem. Soc.* **1998**, *120*, 9718–9719. (d) Jin, S.; Makris, T. M.; Bryson, T. A.; Sligar, S. G.; Dawson, J. H. *J. Am. Chem. Soc.* **2003**, *125*, 3406–3407.
(8) Akhtar, M.; Calder, M. R.; Corina, D. L.; Wright, J. N. *Biochem. J.* **1982**, *201*, 569–580.
(9) Newcomb, D.; Toy, P. H. *Acc. Chem. Res.* **2000**, *33*, 449–455.
(10) Cryle, M. J.; De Voss, J. J. *Angew. Chem., Int. Ed.* **2006**, *45*, 8221–8223.
(11) Sen, K.; Hackett, J. C. *J. Am. Chem. Soc.* **2010**, *132*, 10293–10305.
(12) Porro, C. S.; Sutcliffe, M. J.; de Visser, S. P. *J. Phys. Chem. A* **2009**, *113*, 11635–11642.
(13) Ogliaro, F.; de Visser, S. P.; Cohen, S.; Sharma, P. K.; Shaik, S. *J. Am. Chem. Soc.* **2002**, *124*, 2806–2817.
(14) Kamachi, T.; Shiota, Y.; Ohta, T.; Yoshizawa, K. B. *Chem. Soc. Jpn.* **2003**, *76*, 721–732.
(15) Davydov, R.; Makris, T. M.; Kofman, V.; Werst, D. E.; Sligar, S. G.; Hoffman, B. M. *J. Am. Chem. Soc.* **2001**, *123*, 1403–1415.
(16) Park, M. J.; Lee, J.; Suh, Y.; Kim, J.; Nam, W. *J. Am. Chem. Soc.* **2006**, *128*, 2630–2634.
(17) (a) Chung, L. W.; Li, X.; Sugimoto, H.; Shiro, Y.; Morokuma, K. *J. Am. Chem. Soc.* **2008**, *130*, 12299–12309. (b) Chung, L. W.; Li, X.; Sugimoto, H.; Shiro, Y.; Morokuma, K. *J. Am. Chem. Soc.* **2010**, *132*, 11993–12005.
(18) Capece, L.; Lewis-Ballester, A.; Batabyal, D.; Russo, N. D.; Yeh, S.-R.; Estrin, D. A.; Marti, M. A. *J. Biol. Inorg. Chem.* **2010**, *15*, 811–823.
(19) Emerson, J. P.; Kovaleva, E. G.; Farquhar, E. R.; Lipscomb, J. D.; Que, L., Jr. *Proc. Natl. Acad. Sci. U.S.A.* **2008**, *105*, 7347–7352.
(20) (a) Bollinger, J. M., Jr.; Krebs, C. *Curr. Opin. Chem. Biol.* **2007**, *11*, 151–158. (b) van der Donk, W. A.; Krebs, C.; Bollinger, J. M., Jr. *Curr. Opin. Struct. Biol.* **2010**, *20*, 673–683.
(21) Lundberg, M.; Kawatsu, T.; Vreven, T.; Frisch, M. J.; Morokuma, K. *J. Chem. Theory Comput.* **2009**, *5*, 222–234.
(22) (a) Hirao, H.; Morokuma, K. *J. Am. Chem. Soc.* **2009**, *131*, 17206–17214. (b) Hirao, H.; Morokuma, K. *J. Am. Chem. Soc.* **2010**, *132*, 17901–17909.
(23) Maiti, D.; Fry, H. C.; Woertink, J. S.; Vance, M. A.; Solomon, E. I.; Karlin, K. D. *J. Am. Chem. Soc.* **2007**, *129*, 264–265.
(24) Mukherjee, A.; Cranswick, M. A.; Chakrabarti, M.; Paine, T. K.; Fujisawa, K.; Münck, E.; Que, L., Jr. *Inorg. Chem.* **2010**, *49*, 3618–3628.
(25) Cho, J.; Woo, J.; Nam, W. *J. Am. Chem. Soc.* **2010**, *132*, 5958–5959.
(26) Lee, Y.-M.; Hong, S.; Morimoto, Y.; Shin, W.; Fukuzumi, S.; Nam, W. *J. Am. Chem. Soc.* **2010**, *132*, 10668–10670.
(27) Kunishita, A.; Kubo, M.; Sugimoto, H.; Ogura, T.; Sato, K.; Takui, T.; Itoh, S. *J. Am. Chem. Soc.* **2009**, *131*, 2788–2789.
(28) Lai, W. Z.; Chen, H.; Cho, K.-B.; Shaik, S. *J. Phys. Chem. Lett.* **2010**, *1*, 2082–2087.
(29) Cohen, S; Kozuch, S.; Hazan, C.; Shaik, S. *J. Am. Chem. Soc.* **2006**, *128*, 11028–11029.
(30) Kumar, D; Altun, A.; Shaik, S.; Thiel, W. *Faraday Discuss.* **2011**, *148*, 373–383.
(31) (a) Schlichting, I.; Berendzen, J.; Chu, K.; Stock, A. M.; Maves, S. A.; Benson, D. E.; Sweet, R. M.; Ringe, D.; Petsko, G. A.; Sligar, S. G. *Science* **2000**, *287*, 1615–1622. (b) Note that it is no longer firmly believed that the crystal structure 1DZ9 contains Cpd I. However, in view of the recent results in ref 1, it is not clear anymore that the basis of this disbelief is fully substantiated.
(32) Sherwood, P.; et al. *J. Mol. Struct. (THEOCHEM)* **2003**, *632*, 1–28.
(33) Ahlrichs, R.; Bär, M.; Häser, M.; Horn, H.; Kölmel, C. *Chem. Phys. Lett.* **1989**, *162*, 165–169.
(34) Smith, W.; Forester, T. R. *J. Mol. Graph.* **1996**, *14*, 136–141.
(35) Bakowies, D.; Thiel, W. *J. Phys. Chem.* **1996**, *100*, 10580–10594.
(36) de Vries, A. H.; Sherwood, P.; Collins, S. J.; Rigby, A. M.; Rigutto, M.; Kramer, G. J. *J. Phys. Chem. B* **1999**, *103*, 6133–6141.
(37) MacKerell, A. D., Jr.; et al. *J. Phys. Chem. B* **1998**, *102*, 3586–3616.
(38) (a) Becke, A. D. *Phys. Rev. A* **1988**, *38*, 3098–3100. (b) Lee, C.; Yang, W.; Parr, R. G. *Phys. Rev. B* **1988**, *37*, 785–789. (c) Becke, A. D. *J. Chem. Phys.* **1993**, *98*, 5648–5652. (d) Becke, A. D. *J. Chem. Phys.* **1993**, *98*, 1372–1377.
(39) Hay, P. J.; Wadt, W. R. *J. Chem. Phys.* **1985**, *82*, 299–310.
(40) The LACV3P basis set is a triple-ζ contraction of the LACVP basis set developed and tested at Schrödinger, Inc.
(41) Sharma, P. K.; de Visser, S. P.; Shaik, S. *J. Am. Chem. Soc.* **2003**, *125*, 8698–8699.
(42) Li, C.; Zhang, L.; Zhang, C.; Hirao, H.; Wu, W.; Shaik, S. *Angew. Chem., Int. Ed.* **2007**, *46*, 8168–8170; Corrigendum**2008**, *47*, 8137.
(43) Grimme, S. *J. Comput. Chem.* **2006**, *27*, 1787–1799.
(44) Siegbahn, P. E. M.; Blomberg, M. R. A.; Chen, S.-L. *J. Chem. Theory Comput.* **2010**, *6*, 2040–2044.
(45) Frisch, M. J. et al. *Gaussian 09*, Revision A.02; Gaussian, Inc.: Wallingford CT, 2009.
(46) *Jaguar*, Version 7.6, Schrödinger, LLC: New York, 2008.
(47) Glendening, E. D.; Reed, A. E.; Carpenter, J. E.; Weinhold, F. NBO Version 3.1.
(48) Groves, J. T.; McClusky, G. A.; White, R. E.; Coon, M. J. *Biochem. Biophys. Res. Commun.* **1978**, *81*, 154–160.
(49) Shaik, S.; Kumar, D.; de Visser, S. P.; Altun, A.; Thiel, W. *Chem. Rev.* **2005**, *105*, 2279–2328.
(50) (a) Harris, N.; Cohen, S.; Filatov, M.; Ogliaro, F.; Shaik, S. *Angew. Chem., Int. Ed.* **2000**, *39*, 2003–2007. (b) de Visser, S. P.; Ogliaro, F.; Sharma, P. K.; Shaik, S. *Angew. Chem., Int. Ed.* **2002**, *41*, 1947–1951.

(c) Shaik, S.; Filatov, M.; Schröder, D.; Schwarz, H. *Chem.—Eur: J.* **1998**, *4*, 193–199.
(51) Lonsdale, R.; Harvey, J. N.; Mulholland, A. J. *J. Phys. Chem. Lett.* **2010**, *1*, 3232–3237.
(52) Chen, H.; Ikeda-Saito, M.; Shaik, S. *J. Am. Chem. Soc.* **2008**, *130*, 14778–14790.
(53) Wang, D. Q.; Thiel, W. *J. Mol. Struct. (THEOCHEM)* **2009**, *898*, 90–96.
(54) de Visser, S. P.; Ogliaro, F.; Sharma, P. K.; Shaik, S. *J. Am. Chem. Soc.* **2002**, *124*, 11809–11826.
(55) Huenerbein, R.; Schirmer, B.; Moellmann, J.; Grimme, S. *Phys. Chem. Chem. Phys.* **2010**, *12*, 6940–6948.
(56) Chen, H.; Lai, W. Z.; Shaik, S. *J. Phys. Chem. Lett.* **2010**, *1*, 1533–1540.
(57) Shaik, S.; Wang, Y.; Chen, H.; Song, J.; Meir, R. *Faraday Discuss.* **2010**, *145*, 49–70.
(58) (a) Lonsdale, R.; Harvey, J. N.; Mulholland, A. J. *J. Phys. Chem. B* **2010**, *114*, 1156–1162. (b) Senn, H. M.; Kästner, J.; Breidung, J.; Thiel, W. *Can. J. Chem.* **2009**, *87*, 1322–1337.
(59) (a) Bell, R. P. *Proc. R. Soc. London, Ser. A* **1936**, *154*, 414–429. (b) Evans, M. G. *Trans. Faraday Soc.* **1938**, *34*, 11–24.
(60) Shaik, S.; Lai, W. Z.; Chen, H.; Wang, Y. *Acc. Chem. Res.* **2010**, *43*, 1154–1165.
(61) Mayer, J. M. *Acc. Chem. Res.* **1998**, *31*, 441–450.
(62) Kumar, D.; Karamzadeh, B.; Sastry, G. N.; de Visser, S. P. *J. Am. Chem. Soc.* **2010**, *132*, 7656–7667.
(63) See, for example:Zhang, X.; Schwarz, H. *ChemCatChem* **2010**, *2*, 1391–1394.
(64) Sastri, C. V.; Lee, J.; Oh, K.; Lee, Y. J.; Lee, J.; Jaskson, T. A.; Ray, K.; Hirao, H.; Shin, W.; Halfen, J. A.; Kim, J.; Que, L., Jr.; Shaik, S.; Nam, W. *Proc. Natl. Acad. Sci. U.S.A.* **2007**, *104*, 19181–19186.
(65) (a) Dawson, J. H.; Sono, M. *Chem. Rev.* **1987**, *87*, 1255–1276. (b) Ogliaro, F.; de Visser, S. P.; Shaik, S. *J. Inorg. Biochem.* **2002**, *91*, 554–567.
(66) Altarsha, M.; Benighaus, T.; Kumar, D.; Thiel, W. *J. Am. Chem. Soc.* **2009**, *131*, 4755–4763.
(67) Altarsha, M.; Wang, D. Q.; Benighaus, T.; Kumar, D.; Thiel, W. *J. Phys. Chem. B* **2009**, *113*, 9577–9588.
(68) Murgida, D. H.; Hidebrandt, P. *Acc. Chem. Res.* **2004**, *37*, 854–861.
(69) Ashkenasy, G.; Kalyuzhny, G.; Libman, J.; Rubinstein, I.; Shanzer, A. *Angew. Chem., Int. Ed.* **1999**, *38*, 1257–1261.
(70) Kijac, A. Z.; Li, Y.; Sligar, S. G.; Rienstra, C. M. *Biochemistry* **2007**, *46*, 13696–13703. Note (as proposed by Sligar) that charged lipids can be embedded into the nanodiscs and generate large local fields.
(71) Choi, Y.; Yau, S.-T. *Anal. Chem.* **2009**, *81*, 7123–7126.